

## Effect of the Compaction Platform on the Densification Parameters of Tableting Excipients with Different Deformation Mechanisms

John Rojas\* and Santiago Hernandez

School of Pharmaceutical Chemistry, The University of Antioquia, Medellin 094, Columbia.

Received November 11, 2013; accepted December 12, 2013

Several compaction models have been attempted to explain the compression and compaction phenomena of excipients. However, the resulting parameters could be influenced by the compaction platform such as dwell time, compact mass, geometry and type of material. The goal of this study is to assess the effect of these variables on the densification parameters obtained from key models such as Heckel, non-linear Heckel, Kawakita, Carstensen, and Leuenberger. The relationship among the parameters derived was determined by employing a Principal Component Analysis. Results indicated that factors such as compact geometry, consolidation time and compact mass had a negligible impact on parameters such as tensile strength, yield pressure and compressibility. On the contrary, the excipient type had the largest influence on these parameters. Further, the Leuenberger ( $\gamma$ ) and Carstensen ( $f$ ) parameters were highly correlated and related to the excipient deformation mechanism. Sorbitol and PVP-k30 were the most highly compactable excipients and were characterized for having a low yield pressure ( $P_y$ ), compressibility ( $a$ ), and critical porosity ( $\varepsilon_c$ ). The magnitude of these parameters was highly dependent on the consolidation behavior of each material.

**Key words** deformation mechanism; compaction behavior; compression model; compactibility; tableting performance

The consolidation phenomenon of compressing materials into a cohesive mass during compact formation is a complex process. The pressure applied to bulk pharmaceutical powders give rise to a change in bed density, gradually reducing its volume until a complete tablet is formed. During this process, powders undergo complex transitions and structural changes to form a porous solid. Thus, a final porosity reduction represents a transformation to a new physical irreversible structure where the solid constitute a continuous phase.<sup>1)</sup>

It is commonly accepted that powder consolidation happens by cohesive forces acting at the areas of true interparticle contact points including van der Waals forces, solid bridges and mechanical interlocking. However, only van der Waals forces are significant for tableting of pharmaceutical materials. Hydrogen bonds and electrostatic forces are other examples of forces that act over a distance between particles. Nevertheless, if too much energy is stored elastically at compression, the elastic recovery during decompression could break most of the bonds formed rendering a flaky tablet. For this reason, excipients need to be added to a drug formulation to compensate for intrinsic undesirable properties of the drug.<sup>2,3)</sup>

At the onset of compression, particles within the powder bed are expected to undergo some rearrangement in their packing condition reducing their particle–particle contact distances in which bigger holes between particles are filled with small particles. This process is influenced by surface characteristics, frictional properties and particle size. The smaller the particles, the greater the number of contact points per unit volume.<sup>4)</sup> As the pressure rises, plastic and elastic deformation of the particles occurs, resulting in a reduction of inter/intraparticulate voids forming a coherent mass.<sup>5)</sup> As the pressure increases, particle fracture and rebonding may occur. However, most phases do not follow each other in progression, but overlap each other as the phases of packing and deformation compete concomitantly.<sup>6)</sup>

Several models have been derived to characterize the volume reduction of excipients in the powder bed. Some of them were obtained from empirical mathematical relationships where different mechanisms occur at distinct ranges of applied pressure.<sup>7,8)</sup> For instance, the Kawakita model is useful for materials that undergo a significant volume reduction at the initial stage of compression.<sup>9)</sup> This model is expressed as:

$$\frac{P}{1 - (v_n/v_i)} = \frac{1}{a \cdot b} + \frac{P}{a} \quad (1)$$

Where,  $v_n$ ,  $v_i$ ,  $P$ ,  $a$ , and  $b$  correspond to the tablet volume, initial apparent volume, compression pressure, compressibility index and forces opposing to compression, respectively.<sup>10,11)</sup> On the other hand, the Heckel, Carstensen, and nonlinear Heckel models are based on the percolation theory which establishes that consolidation occurs by several percolation stages. The first one is the formation of structured compacts by particle rearrangement. At the 2nd stage, volume reduction occurs by changing particle shape due to by fragmentation/plastic deformation. The third stage is reached when the remaining porosity is reduced to a degree that pores do not percolate anymore.<sup>12)</sup> The Heckel model relates the powder porosity as a function of the compression pressure. It is based on the assumption that compression is a first order reaction, in which porosity is the reagent and densification the product.<sup>13)</sup> The Heckel model assumes that consolidation occurs in three phases. Phase I represents fragmentation/rearrangement of particles in the powder bed. Phase II is the linear portion of the curve where plastic deformation takes place. On the contrary, phase III correspond to the expansion of the tablet height due the increase in porosity at the decompression stage. The linear region of the curve is expressed as:

$$-\ln(\varepsilon) = kP + A \quad (2)$$

Where,  $\varepsilon$ ,  $P$ ,  $A$ , and  $k$  correspond to the compact porosity,

The authors declare no conflict of interest.

\* To whom correspondence should be addressed. e-mail: jrojasca@gmail.com

compaction pressure, intercept and slope, respectively. The inverse of the slope represents the mean yield pressure of a material. At this pressure, a plastic deformation takes place. This parameter is also used to determine the consolidation mechanism of materials. From the value of intercept ( $A$ ) the total initial relative density by die filling and particle rearrangement is obtained.

Leuenberger developed a modified non-linear Heckel model which takes into account the relationship between the susceptibility to pressure and relative density of the material in a low and high pressure range altogether:

$$P = \frac{1}{C} \left[ \rho_c - \rho(1 - \rho_c) \ln \left( \frac{1 - \rho}{1 - \rho_c} \right) \right] \quad (3)$$

Where,  $C$  represents the ability of the material to deform by a plastic mechanism. A large value of  $C$  indicates a large plasticity. Further, the critical solid fraction ( $\rho_c$ ) or powder porosity ( $\varepsilon_c$ ) indicates the point where powder rearrangement causes a mechanical rigidity to form a stable compact. Beyond this  $\rho_c$  or below  $\varepsilon_c$  a coherent compact is formed.<sup>12)</sup> The Carstensen model, on the other hand, assumes that porosity decreases exponentially with pressure, and in the range of pharmaceutical pressures porosity tends to a non-zero value. This means that at infinite pressure a compact keeps some residual porosity.<sup>14)</sup> The model is expressed as:

$$\frac{1}{1 - \varepsilon} = V_s \cdot D + V_a \cdot D \cdot \exp^{-fP} \quad (4)$$

Where,  $\varepsilon$ ,  $V_s$ ,  $V_a$ ,  $D$ ,  $f$  and  $P$  corresponds to porosity, volume of powder and volume at high pressure ranges, true density, compressibility and compression pressure, respectively. Since the previous models do not include a prediction of compact strength, semilogarithmic plots of compact tensile strength vs. solid fraction have been developed. However, only at low solid fractions they appear to be linear rendering unrealistic values for non-porous excipients. Therefore, the use of the non-linear Leuenberger model, which is also based on the percolation theory, must be considered. This model relates compact tensile strength and the product of compaction pressure and solid fraction as follows<sup>12)</sup>:

$$\sigma_t = T_{\max}(1 - e^{-\gamma P}) \quad (5)$$

Where;  $\sigma_t$ ,  $T_{\max}$ ,  $\gamma$ ,  $\rho$ , and  $P$  correspond to the compact tensile strength, maximum tensile strength, compression susceptibility, solid fraction, and compression pressure, respectively. A high value of compression susceptibility indicates a limiting value of tensile strength and a sharp decrease in compact porosity may be attained at a relatively low compression pressure.<sup>15)</sup>

Currently, no systematic research has been conducted to investigate the effect of key compaction factors on the densification parameters obtained from these models.<sup>16)</sup> Therefore, the goal of this study is to apply a multivariate analysis to assess the effect of tablet mass, geometry, consolidation time, and excipient type on parameters derived from compressibility (Kawakita, Heckel, non-linear Heckel, and Carstensen) and compactibility (Leuenberger) models used to characterize the consolidation behavior of powders.

## Experimental

This study employs representative excipients used for direct compression, wet granulation and roller compaction of drugs. MCC PH101 (Avicel, lot 6N608C) was obtained from FMC BioPolymers. Lactose monohydrate (lot 5720927003-001-020) and sorbitol (lot SP15122011) were purchased from Saputo ingredients and Roquette, respectively. Calcium diphosphate (lot BCU250711) and polyvinyl pyrrolidone (lot P1109011-1) were obtained from Bell Chem international. Pregelatinized starch (lot IN504089) was purchased from Colorcon. All materials were used as received.

**Powder Porosity** A helium displacement micropycnometer (AccuPyc II 1340, Micromeritics Corp., Norcross, GA, U.S.A.) was employed. It was calculated by subtracting the unity from the ratio of bulk density and true density.

**Preparation of Compacts** Cylindrical and convex compacts of about 100, 200, 400, and 500mg were made at a dwell time of 1 and 30s. Each excipient was poured onto a 6.5mm and 13mm flat and convex faced punch-and-die tooling and compressed on a single punch tablet press (060804 Compac, Indemec, Itagüi-Columbia) at pressures from *ca.*10 to 200MPa. The upper punch was equipped with a load cell (LCGD-10K, Omega Engineering, Inc., Stamford, CT, U.S.A.) and a strain gauge meter (DPiS8-EI, Omega Engineering, Inc.). The relative humidity of the environment was controlled below 50%. Compacts were analyzed immediately after ejected.

**Compact Porosity** Compact thickness and diameters were measured with an electronic digital caliper (Titer; measuring range 0–150mm and readability of 0.01mm). The tablet thickness was measured at three different points around the compact and the average was taken. The volume of the cylindrical compacts at a given pressure was calculated from:

$$V = \pi r^2 h \quad (6)$$

Where,  $V$ ,  $r$ , and  $h$  are the volume, radius and thickness of the compact, respectively. On the other hand, the volume of the convex-faced tablet was found by:

$$V = \left[ 2 \frac{\pi h}{6} (3r^2 + h^2) + [2\pi r^2 w] \right] \quad (7)$$

Where,  $h$ ,  $r$ , and  $w$  correspond to the height of the curved section of the tablet, radius and height of the cylindrical section of the tablet, respectively. The apparent density of the compact was calculated by dividing the tablet mass by its volume. Compact porosity ( $\varepsilon$ ) was calculated from:

$$\varepsilon = 1 - \frac{\rho_{\text{app}}}{\rho_{\text{true}}} \quad (8)$$

Where,  $\rho_{\text{app}}$  is the apparent density of the compact and  $\rho_{\text{true}}$  is the true density of the material. The ratio of  $\rho_{\text{app}}/\rho_{\text{true}}$  is a measurement of the solid fraction of the compact.

**Compact Tensile Strength** The radial tensile strength (TS) was obtained according to the Fell and Newton and Pitt equations for cylindrical and concave compacts, respectively. The data of crushing strength values obtained on a hardness tester (U.K. 200, Vankel, Manasquan, NJ, U.S.A.) were transformed to tensile strength and used in the Leuenberger model.<sup>17)</sup>

**Principal Component Analysis (PCA)** PCA is a type of multivariate analysis that identifies patterns in data and expresses them in such a way as to highlight their similarities and differences in three main axes (PC1, PC2, and PC3). The patterns are the lines that most closely describe the relationships between the data. The PC1 vector is the direction on the abscissa along which projections that have the largest variance. The PC2 is the direction, which maximizes variance among all directions orthogonal to the PC1. The Minitab® software (v.16, Minitab®, State College, U.S.A.) was used for the PCA data analysis. The independent variables were excipient type (Pregelatinized starch, MCC PH101, calcium diphosphate, lactose monohydrate, PVP-k30, and sorbitol), compact geometry (cylindrical and convex) and consolidation time (1, 30s). The responses variables were obtained from the parameters obtained from the Heckel ( $P_y$ ), Kawakita ( $a$  and  $b$ ), non-linear Heckel ( $\epsilon_c$  and  $C$ ), Carstensen ( $V_s$ ,  $V_a$  and  $f$ ), and Leuenberger (area under the curve ( $AUC$ ),  $T_{max}$  and  $\gamma$ ) parameters.

**Results and Discussion**

In this study, the PC1, PC2, and PC3 had a variance of 4.98, 3.20, and 1.40 respectively, and accounted for ca.64% of the total variance indicating that most data structure was captured into the three underlying dimensions studied. The loading plot of measured properties is shown in Fig. 1. The lines show projections of the compaction factors and the resulting parameters from the models onto the PC1, PC2, and PC3 in a 3D plot. The loadings can be understood as weights for each original property when calculating the principal component. This plot is the result of the linear combination of original data that maximizes data variance. Further, each point in the graph indicates the contribution of this property in defining these components. Tableting factors contributing very little to the components such as dwell time and compact geometry had small loading values and appear plotted near the center. These factors had virtually no effect on the overall behavior of the parameters studied. As a consequence, the plastic deformation due to a reduction in the time available for stress relaxation and bond formation did not affect compactibility. Thus,

prolongation of the time available for deformation did not increase tablet densification. Compact mass had a moderate influence on these parameters. On the other hand, the excipient type along with all other parameters had large linear components and appear dispersed around the borders of the plot suggesting the excipient type was the most important variable that affected all densification parameters.

The data set obtained from the Leuenberger and Carstensen models formed a cluster and are depicted closed to the excipient vector indicating they are highly correlated. In other words, their parameters mainly depended on the type of excipient used. On the contrary, parameters derived from the non-linear Heckel model ( $\epsilon_c$  and  $C$ ) and the compressibility index ( $a$ ) obtained from the Kawakita model were almost directly opposite to the excipient vector indicating an inverse correlation. Furthermore, some pairs such as  $f$  and  $\gamma$ ,  $AUC$ , and  $T_{max}$ ,  $\epsilon_c$  and “ $a$ ,”  $V_s$ , and  $V_a$  were also correlated. On the contrary,  $AUC$  and  $T_{max}$  were inversely correlated with  $\epsilon_c$ . The scores for PC1 and PC2 are:

$$PC1 = 0.28Exc + 0.007Geom + 0.021Time + 0.044Mass + 0.4AUC + 0.28T_{max} + 0.38\gamma - 0.35P_y - 0.19a + 0.14b + 0.30V_s + 0.23V_a + 0.40f - 0.26\epsilon_c - 0.04C$$

$$PC2 = 0.29Exc - 0.05Geom + 0.04Time + 0.10Mass - 0.13AUC - 0.29T_{max} + 0.08\gamma + 0.22P_y - 0.26a + 0.39b - 0.15V_s - 0.38V_a + 0.02f - 0.39\epsilon_c - 0.43C$$

The PC1 model represents a direct relationship between the excipient type and the Leuenberger ( $T_{max}$ ,  $AUC$ , and  $\gamma$ ) and Carstensen ( $V_s$ ,  $V_a$ , and  $f$ ) parameters. On the other hand, the modified Heckel parameters ( $\epsilon_c$  and  $C$ ) showed a negative effect with the excipient type. The PC2 component on the other hand, showed a relationship between excipient, yield pressure and the “ $b$ ” Kawakita constant, being this opposite with all other parameters. Further, the effect of compact mass and time on these parameters can be considered as negligible.

Figure 2 shows the 3D PCA score plot for the tableting conditions and parameters studied. The score plot of the three

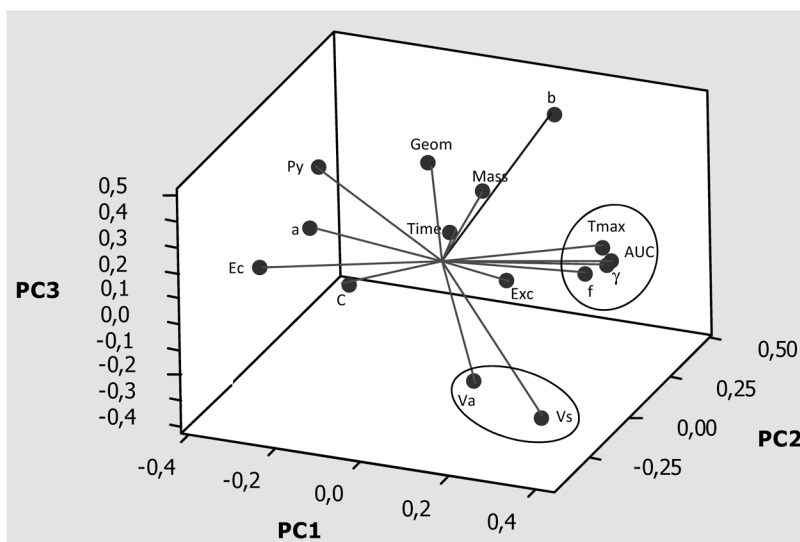


Fig. 1. Loading Plot of the Effect of Tableting Conditions on Parameters Resulted from the Heckel, Kawakita, Non-linear Heckel, Carstensen, and Leuenberger Models

principal components contains the original data in a rotated coordinate system. This plot was able to classify and mainly attribute data variability to the excipient type. The first component separates PVP-k30 and sorbitol from calcium diphosphate, lactose monohydrate and MCC PH101. Since the PC1 was mainly influenced by the Leuenberger and Carstensen parameters, data stratification was mainly dependent on the excipient compactibility. For this reason, highly compactable excipients are illustrated on the right side of the PC1 axis, whereas poorly compactable excipients are shown on the left side. Moreover, these highly compactable excipients were also

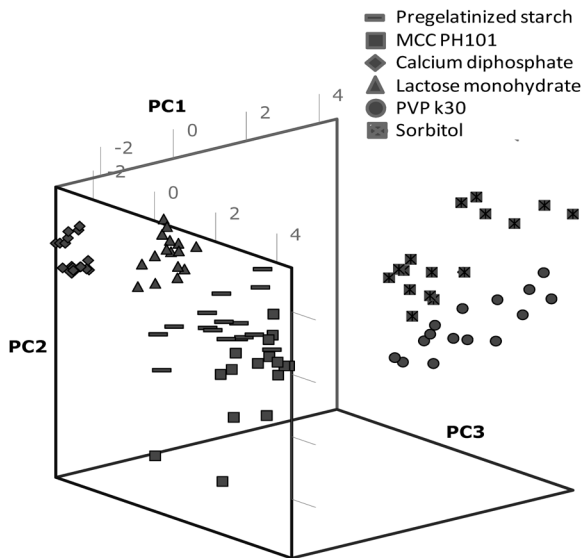


Fig. 2. PCA Score Plot of the Effect of Tableting Conditions on Parameters Obtained from the Heckel, Kawakita, Non-linear Heckel, Carstensen, and Leuenberger Models

characterized for having a low yield pressure ( $P_y$ ), compressibility ( $a$ ), critical porosity ( $\epsilon_c$ ), and deformation constant ( $C$ ).

The PC2 and PC3 separated calcium diphosphate and lactose monohydrate from MCC PH101 and pregelatinized starch, whereas they partially overlapped the data set of sorbitol and PVP-k30. In this case, excipient stratification was essentially due to plasticity as reflected on the powder yield pressure ( $P_y$ ) obtained from the Heckel model and the “ $b$ ” constant derived from the Kawakita model. This was translated in a high and low  $P_y$  “ $b$ ” values for brittle and plastic deforming excipients, respectively. Further, plasticity of sorbitol and PVP-k30 was high and comparable as indicated by the partial overload of their data set.

The correlation matrix among the parameters studies is shown in Fig. 3. A good correlation is depicted as a straight line with either a positive or negative slope. Conversely, a horizontal line or a cluster formation indicates no correlation. There was a good correlation between compactibility (indicated as  $AUC$ ) and  $T_{max}$  ( $r^2=0.7282$ ). As a result, materials having a large compact tensile strength such as sorbitol and PKP k30 are expected to have a large tensile strength at infinite compression pressure and hence, a large compactibility determined by taking the  $AUC$  from the Leuenberger plot. Likewise, the “ $f$ ” and “ $\gamma$ ” parameters from the Carstensen and Leuenberger models were correlated ( $r^2=0.6571$ ) suggesting that both parameters were related to the plasticity of the material. For instance, sorbitol had the largest “ $f$ ” and “ $\gamma$ ” values indicating a large ductility, whereas very low values were obtained for calcium diphosphate and lactose indicating a predominant brittle character. The critical porosity ( $\epsilon_c$ ) and deformation parameter ( $C$ ) from the non-linear Heckel model presented some correlation ( $r^2=0.6446$ ). In this case,  $C$  and  $\epsilon_c$  were very high for plastic deforming excipients indicating that a compact of good strength and plasticity can be achieved

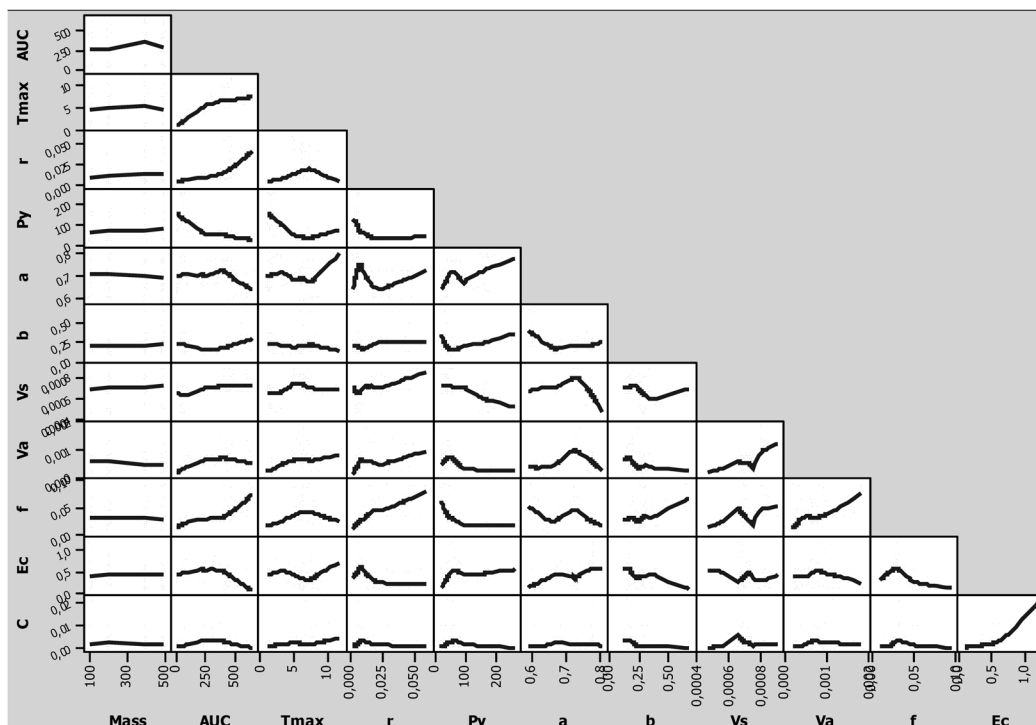


Fig. 3. Correlation Matrix among the Densification Parameters



at high porosities. Further, the  $V_a$  and  $V_s$  parameters from the Carstensen model showed a small correlation ( $r^2=0.4620$ ). In this case,  $V_s$  was equal or larger than  $V_a$  indicating that the volume reduction of the solid was larger in magnitude in relation to the reduction in volume at low compression forces, which still contains interparticle/extraparticle voids.

Figure 4 depicts the compressibility plots resulted from the Heckel, Kawakita, non-linear Heckel, and Carstensen models. All these models showed the same trends, but the amplitude of densification in each model differs from each other. For instance, the densification data range depicted in the Heckel and non-linear Heckel models was wider than that of Kawakita and Carstensen models. For this reason, the first two models were preferred to detect small differences in powder consoli-

dation among several excipients. In general, sorbitol and calcium diphosphate were the excipients that exhibited the largest and smallest densification upon compression, respectively. Further, these two materials presented the largest plastic deformation ability and the most brittle character, respectively as indicated by their low yield pressure (Table 1). A mean yield pressure ( $P_y$ ) below 80MPa is considered an indication of plastic deformation.<sup>18)</sup> In this study, factors such as consolidation time, compact geometry and compact mass showed no influence on the powder yield pressure. On the contrary, the most salient factor that affected all parameters was the excipient type. Further, sorbitol and calcium diphosphate also exhibited the largest and smallest Kawakita slope, respectively. This is translated in large and small volume reduction, respectively.

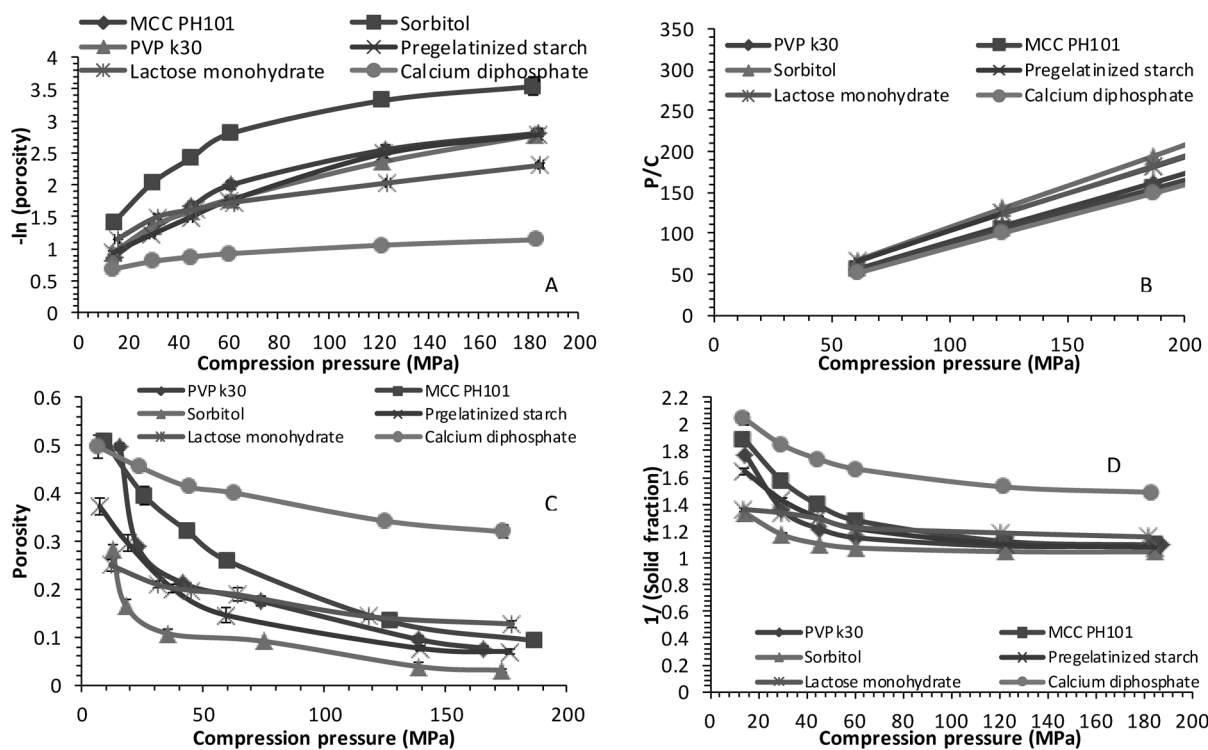


Fig. 4. Comparison of the Different Powder Consolidation Models: A=Heckel, B=Kawakita, C=Nonlinear Heckel, D=Carstensen  
Each point represents the average of 16 measurements.

Table 1. Densification Parameters for Each Excipient (n=16)

Par.	Lactose monohydrate	Calcium diphosphate	Pregelatinized starch	MCC PH101	PVP-k30	Sorbitol
$\epsilon$ (%)	60.0	65.0	56.0	77.0	72.0	70.0
AUC (MPa <sup>2</sup> )	19±3	57±5	204±114	397±64	507±87	532±68
$T_{max}$ (MPa)	1.0±0.1	1.7±0.6	4.2±1.6	9.1±1.7	6.1±0.8	7.3±1.0
$\gamma$ (MPa <sup>-1</sup> )	0.003±0.001	0.005±0.002	0.010±0.000	0.010±0.000	0.036±0.015	0.028±0.010
$P_y$ (MPa <sup>-1</sup> )	117±39	201±43	54±14	59±11	33±11	28±4
$a$ (%)	65.0±2.0	78.0±2.0	67.0±1.0	77.0±1.0	73.0±1.0	60.0±1.0
$b$	0.21±0.03	0.30±0.05	0.15±0.05	0.16±0.01	0.22±0.06	0.41±0.18
$V_s$ (cm <sup>3</sup> )	0.0007±0.0000	0.0005±0.0000	0.0007±0.0000	0.0007±0.0000	0.0008±0.0000	0.0007±0.0000
$V_a$ (cm <sup>3</sup> )	0.0002±0.0000	0.0002±0.0001	0.0006±0.0001	0.0007±0.0001	0.0011±0.0003	0.0004±0.0002
$f$ (MPa <sup>-1</sup> )	0.02±0.01	0.02±0.00	0.03±0.01	0.03±0.00	0.06±0.02	0.06±0.02
$\epsilon_c$ (%)	37.0±8.0	54.0±2.0	53.0±1.4	74.0±2.2	71.0±1.9	78.0±1.3
$C$ (MPa <sup>-1</sup> )	0.001±0.001	0.001±0.000	0.004±0.000	0.007±0.006	0.002±0.001	0.002±0.003
$d_g$ (µm)	104±94	182±10	55±15	86±14	96±9	191±9

Par.=Parameter,  $\epsilon$ =powder porosity,  $T_{max}$ =tensile strength at infinitive compression pressure,  $\gamma$ =compression susceptibility,  $P_y$ =powder yield pressure,  $a$ =compressibility index,  $b$ =cohesive forces opposing to compression,  $V_s$ =volume reduction of the solid at infinite compression,  $V_a$ =volume reduction at infinite pressures,  $f$ =compression parameter,  $\epsilon_c$ =critical porosity,  $C$ =nonlinear Heckel compression constant,  $d_g$ =geometric mean diameter.

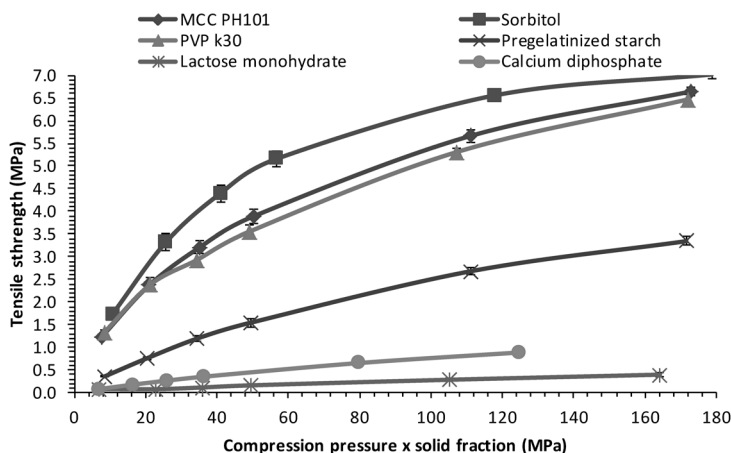


Fig. 5. Leuenberger Plots Showing Excipient Compactibility

Each point represents the average of 16 measurements.

The inverse of the “*b*” constant which represents the resistant cohesive forces to volume reduction was the smallest for sorbitol and calcium diphosphate indicating that large particles move and rearrangement in the powder bed better than materials having particle sizes smaller than  $100\mu\text{m}$  (lactose monohydrate, PVP-k30, MCC PH101, and pregelatinized starch).

The non-linear Heckel model was derived from the percolation theory, which describes the interconnectivity of various regions of the compression system. This model shows a decrease in porosity (entrapped air) of materials with increasing pressures (Fig. 4C). The critical porosity depended on the type of excipient employed. As observed in the non-linear Heckel plot, calcium diphosphate had the least volume reduction ability with compression pressure and sorbitol had the largest one. Moreover, MCC PH101 and PVP-k30, which were the materials with the largest powder porosity, also presented the largest change of porosity at low compression pressures (ca. 15–40 MPa). This phenomenon was more intense for highly plastic deforming excipients such as sorbitol and PVP-k30 at all compression pressures. Therefore, sorbitol, PVP-k30 and MCC PH101 exhibited the largest compressibility constant (*C*) and critical porosity ( $\epsilon_c$ ), below such value a coherent compact is formed. As a result, these two materials need low compression forces to transform a powder into a cohesive compact.

The Carstensen model is represented as the inverse of the solid fraction as a function of compression pressure (Fig. 4D). The excipient plots follow the same trends as discussed previously. The change of solid fraction reached a plateau for most excipients at 60 MPa. Beyond this pressure, porosity, represented as void spaces ( $V_a$  and  $V_v$ ) remained almost unchanged. This is attributed to the assumption that at infinite compression pressure there is always some residual porosity. Therefore, for most excipients and especially plastic deforming materials very low compression pressures were needed to reach these parameters.

The Leuenberger plots are depicted in Fig. 5. These curves give a general description of the compactibility process. Leuenberger classified materials according to the magnitude of the compressibility parameter ( $\gamma$ ) and established plastic deforming materials as those having an “ $\gamma$ ” value  $\geq 0.01\text{ MPa}^{-1}$ . In this scenario, sorbitol and PVP-k30 were considered as highly plastic deforming excipients presenting also a high compactibility as indicated by their large area under the

curve (*AUC*) and  $T_{\text{max}}$  values. Therefore, it is expected these materials to absorb energy easily preventing the accumulation of elastic stress for crack growth and brittle separation of particles resulting in a compact of high strength. On the other hand, brittle deforming excipients such as calcium diphosphate and lactose monohydrate presented a very small compactibility and their profiles were almost linear. As a result, when their particles were under stress at the edge of contact areas a crack propagation resulted in compacts with a low tensile strength.

## Conclusion

The tableting platform such as compact geometry, consolidation time and compact mass had a negligible influence on the densification parameters obtained from the compression and compaction models as compared to the effect of excipients. The Leuenberger ( $\gamma$ ) and the Carstensen (*f*) parameters were highly correlated and indicated the consolidation mechanism of materials. Sorbitol and PVP-k30 were the most highly compactable excipients and were characterized for having a low yield pressure ( $P_y$ ), compressibility (*a*), critical porosity ( $\epsilon_c$ ), and plasticity parameter (*C*). There was a good correlation between compactibility (*AUC*) and  $T_{\text{max}}$  indicating that materials having a large compact tensile strength are expected to have a high compactibility.

**Acknowledgment** We greatly thank the committee for the development of research (CODI) and its sustainability strategy (2013–2014) for their financial support.

## References

- 1) Fassihi A. R., *Int. J. Pharm.*, **44**, 249–256 (1988).
- 2) Gabaude C. M., Guillot M., Gautier J. C., Saudemon P., Chulia D., *J. Pharm. Sci.*, **88**, 725–730 (1999).
- 3) Hamid S. M., “Thesis of Ph.D. degree.” University of Basel, Switzerland, p 253, 2011.
- 4) Michrafy A., Ringenbacher D., Tchoreloff P., *Powder Technol.*, **127**, 257–266 (2002).
- 5) Patel S., Kaushal A. M., Bansal A. K., *Pharm. Res.*, **24**, 111–124 (2006).
- 6) Sørensen A. H., Sonnergaard J. M., Hovgaard L., *Pharm. Dev. Technol.*, **10**, 197–209 (2005).
- 7) Wu C.-Y., Ruddy O. M., Bentham A. C., Hancock B. C., Best S. M., Elliott J. A., *Powder Technol.*, **152**, 107–117 (2005).
- 8) Wu J. S., Ho H. O., Sheu M. T., *Powder Technol.*, **118**, 219–228

- (2001).
- 9) Nicklasson F., Alderborn G., *Pharm. Res.*, **17**, 949–954 (2000).
  - 10) Denny P. J., *Powder Technol.*, **127**, 162–172 (2002).
  - 11) Yamashiro M., Yuasa Y., Kawakita K., *Powder Technol.*, **34**, 225–231 (1983).
  - 12) Hadzovic E., “Thesis of Ph.D. degree.” University of Basel, Switzerland, 2008, pp. 19–22.
  - 13) Ilkka J., Paronen P., *Int. J. Pharm.*, **94**, 181–187 (1993).
  - 14) Cartensen J. T., Geoffroy J. M., Dellamonica C., *Powder Technol.*, **62**, 119–124 (1990).
  - 15) Jetzwer W., Leuenberger H., Sucker H., *Pharm Technol.*, **74**, 33–39 (1983).
  - 16) Kiekens F., Debunne A., Vervaeet C., Baert L., Vanhoutte F., Van Assche I., Menard F., Remon J. P., *Eur. J. Pharm. Sci.*, **22**, 117–126 (2004).
  - 17) Haririan I., Newton J. M., *DARU*, **7**, 36–37 (1999).
  - 18) York P., *Drug Dev. Ind. Pharm.*, **18**, 677–721 (1992).